1-1-2019

Coupling Numerical Analysis of Vibration and Thermal Buckling of an Automotive Brake Disc

Joseph-shaahu Shaahu
University of Denver

Coupling Numerical Analysis of Vibration and Thermal Buckling of an Automotive Brake Disc

Abstract

An engaged brake system generates high temperature gradients in the brake rotor and brake pads. This high temperature gradient in turn induces thermal buckling. During high speed rotation, vibration is likely to occur in the system. In terms of a brake disc vibration will occur when there is a misalignment of the brake disc or thermoelastic instability (hot spot) forms on the brake rotor. Coupled and uncoupled problems of thermal buckling and vibration of a brake disc are analyzed and presented using finite element analysis in this paper. Thermal buckling depends on the direction of the high temperature gradient. Having the temperature distributed either in the radial direction or axial direction affects the critical buckling load, which shows a noticeable change in the buckling temperature. Effects of vibration on thermal buckling and effects of the buckling temperature on vibration were analyzed as the coupling analysis of vibration and thermal buckling. In a simplified thermal buckling study, the thermal loading conditions were linear, sinusoidal and exponential temperature profiles distributed increasingly in the radial direction with the minimum temperature at the inner radius and maximum temperature at the outer radius. Each temperature profile had a constant temperature change of 228°C. Uniform temperatures were assumed in the axial and circumferential directions.

Document Type

Thesis

Degree Name

M.S.

Department

Mechanical Engineering

First Advisor

Yun-Bo Yi, Ph.D.

Second Advisor

Mohammad A. Matin, Ph.D.

Keywords

Thermal buckling, Thermoelastic instability (hot spot), Brake disc

Subject Categories

Engineering | Mechanical Engineering

Coupling Numerical Analysis of Vibration and Thermal Buckling of an Automotive Brake Disc

A Thesis

Presented to

the Faculty of the Daniel Felix Ritchie School of Engineering and Computer Science

University of Denver

In Partial Fulfillment

of the Requirements for the Degree

Master of Science

by

Joseph-shaahu Shaahu

November 2019

Advisor: Dr. Yun-Bo Yi

Author: Joseph-shaahu Shaahu
Title: Coupling Numerical Analysis of Vibration and Thermal Buckling of an Automotive Brake Disc
Advisor: Dr. Yun-Bo Yi
Degree Date: November 2019

ABSTRACT

An engaged brake system generates high temperature gradients in the brake rotor and brake pads. This high temperature gradient in turn induces thermal buckling. During high speed rotation, vibration is likely to occur in the system. In terms of a brake disc vibration will occur when there is a misalignment of the brake disc or thermoelastic instability (hot spot) forms on the brake rotor. Coupled and uncoupled problems of thermal buckling and vibration of a brake disc are analyzed and presented using finite element analysis in this thesis. Thermal buckling depends on the direction of the high temperature gradient. Having the temperature distributed either in the radial direction or axial direction affects the critical buckling load, which is noticed in the buckling temperatures. Effects of vibration on thermal buckling, and effects of the buckling temperature on vibration were analyzed as the coupling analysis of vibration and thermal buckling. In a simplified thermal buckling study, linear, sinusoidal and exponential temperature profiles are chosen for the thermal loading condition. The temperature increases in the radial direction with the minimum temperature at the inner radius and maximum temperature at the outer radius. Each temperature profile had a constant temperature change of 228°C. Uniform temperature was assumed in the circumferential directions.

ACKNOWLEDGMENTS

I want to thank my advisor Dr. Yun-Bo Yi for his guidance, invaluable support, and advice I received from him and overall his patience throughout my thesis process and my master's degree.

I also would like to thank my parents and brother for their support, faith in me and encouragement throughout my education. Also, I want to thank all those who supported me and encouraged my pursuit of higher education.

TABLE OF CONTENTS

LIST OF FIGURES

LIST OF TABLES

CHAPTER ONE: INTRODUCTION

1.1 Brake System Introduction

Newton's first law of motion states every body perseveres in its state of being at rest or of moving uniformly straight forward except insofar as it is compelled to change its state by forces impressed [1]. A body compelled to change its state when in motion is seen as that body coming to a stop. The force impressed on it (external force) can be another body obstructing its motion or friction. A body is not capable of being in motion indefinitely; there is always friction to slow down the body to an eventual stop. Friction is resistance to sliding. Any two objects in contact with and trying to move relative to each other have friction [3]. Over the years, friction has been studied and used to create the external force exerted on a body in motion to change its state. The process of using friction to create a force to stop a moving body especially a vehicle is called braking.

A brake is an essential safety mechanism in any moving vehicle in production today such as cars, airplanes, and trains. A brake's function is to slow or bring to a complete stop a moving vehicle. An assembly of a brake system showing its components is shown in Figure 1-1.

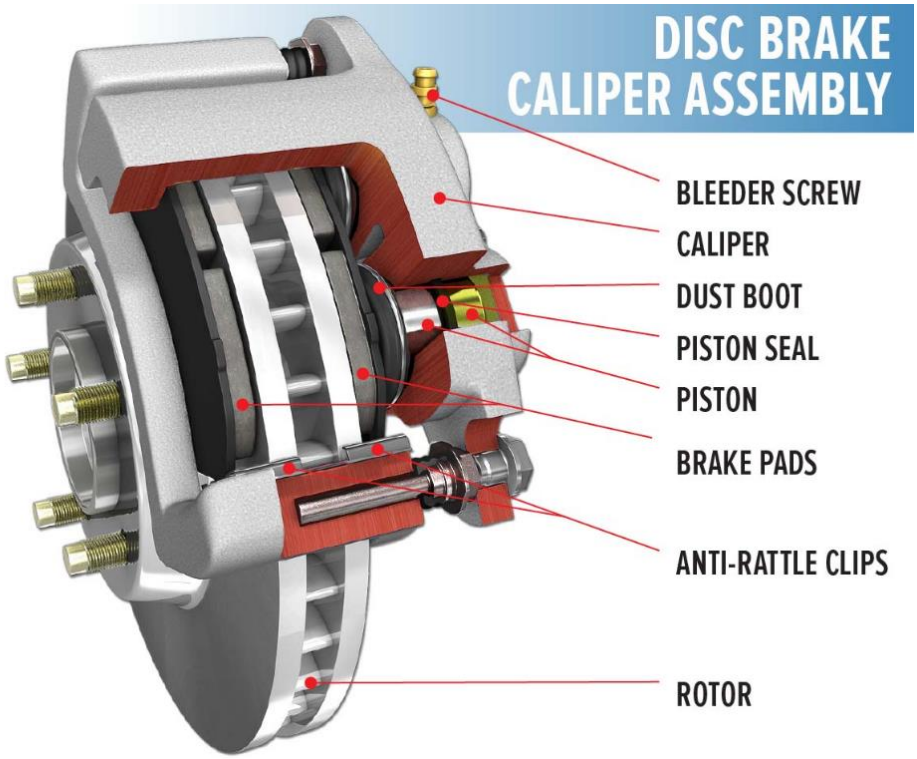

Figure 1-1: Disc brake assembly [21]

For the purpose of this thesis, only three components will be discussed, as these are also known as the main components in the brake assembly. The three components are the rotor, caliper and brake pads. The brake pads are housed in the caliper along with a piston and are located on either side of the rotor. The rotor rotates with the wheels, while the caliper and every other component housed in the caliper including the brake pads are fixed in place and do not rotate with the wheels.

The working principle of a hydraulic brake system is shown in Figure 1-2. When the brake pedal is pushed the brake fluid gets compressed inside the master cylinder and that in turn applies pressure to the piston housed in the caliper. The piston also applies

pressure to the brake pads and the pads clamp down on the disc rotor gradually preventing it from rotating. During the braking process, heat is generated. The heat generated is due to the sliding friction between the brake pads and the rotor. This heat generated can cause a temperature change which in some cases can be really high depending on the angular velocity of the disc rotor, the pressure applied by the brake pads, and the friction material.

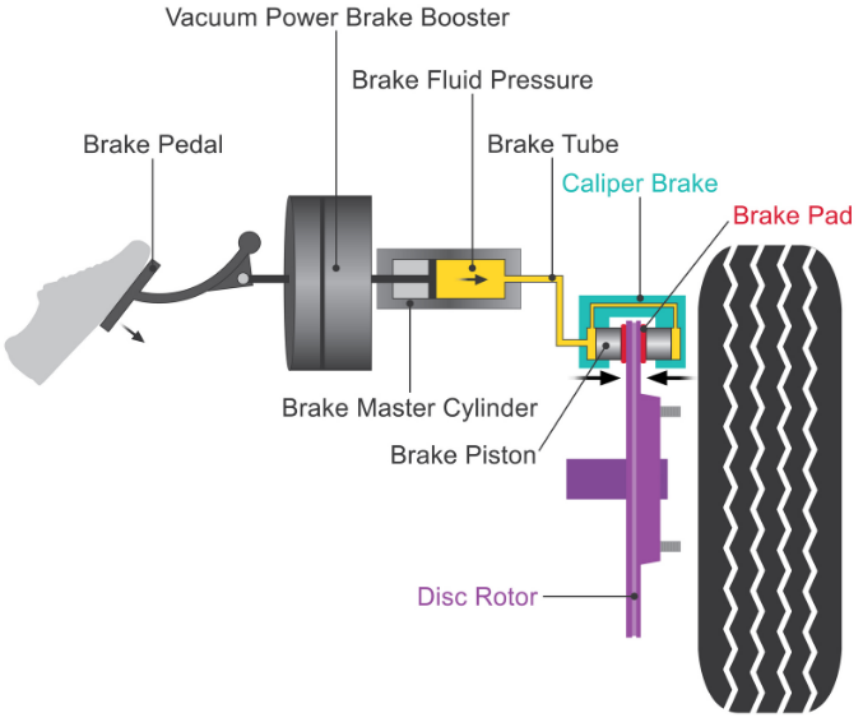

Figure 1-2: Working principle of a hydraulic brake system [22]

1.2 Thesis Description and Background

Thermal buckling is a well known problem and continuous research topic in the automotive industry today. Buckling is an instability that leads to structural failure. Buckling load is the load at which the current equilibrium state of a structural element or structure suddenly changes from stable to unstable, and is, simultaneously, the load at which the equilibrium state suddenly changes from that previously state configuration to another stable configuration with or without an accompanying large response (deformation or deflection) [8]. Several literatures, publications, and analyses have been published for brake disc to be able to design a reliable brake disc for automobiles and ensure the safety of automobile users. Analysis such as thermal, structural and squeal have been extensively researched. During braking, it is known that heat generated in the process is due to friction. The heat generated in the process raises the temperature non-uniformly in the brake rotor and brake pads. These temperatures can sometimes get as high as 800°C. The high temperatures may induce thermal stresses due to thermal expansion in the rotor and lead to thermal buckling. Simplified forms of a thermal buckling problem have been studied with different types of temperature profiles simulated to get a better understanding of the effects of thermal buckling in automotive systems such as clutches and brake discs.

This thesis is a study of uncoupled thermal buckling with simulated temperature profiles and a coupling analysis of vibration and thermal buckling. The coupling study is a two-step process. First, utilizing ANSYS, a vibration simulation is run, and the

deformation result is obtained. Second, utilizing a correlation between mechanical deformation and thermal expansion, a temperature change is obtained using MATLAB. The temperature change obtained is used as the basis for the temperature gradient (profile) in the thermal buckling simulation. There are different types of vibration to consider for the coupling study. In the case of this thesis, vibration caused by rotation is used as a basis for the coupling with thermal buckling. The distribution of the contact pressure is affected if there is axial deformation during the rotation of the brake rotor. This in turn affects the temperature gradient during the generation of heat due to friction and affects the thermal buckling critical load. The coupling study of vibration and thermal buckling is then compared with the uncoupled thermal buckling study to understand how much the presence of vibration affects the thermal buckling critical temperature of the brake rotor.

CHAPTER TWO: LITERATURE REVIEW

2.1 Review of Vibration Study

Vibration was introduced in the early millennium BC. It came as a result of the base sciences in which it was derived from, mechanics and mathematics. Vibration is always used to describe wave and sounds. Over the years vibration have been used to study and quantitate a systems equilibrium state. Such simplified systems are often represented with a mass and spring system. Fred [15] indicated that although it would be reasonable to assume a vibrating system is out of balance the amplitude of a frequency determines the severity of a fault. In reality, vibrating systems or bodies are not necessarily out of balance. Every body vibrates at a certain frequency; this frequency is known as the natural frequency of the body. Vibration can be considered a sub-branch of dynamics and the study and understanding of vibration is very versatile branch of science. These studies have shown to be capable of predicting earthquakes and aided in the design of structures to withstand these vibrations. Boughner [16] used low frequency vibration to study the effect on arterial walls in regions where a murmur may occur. Low frequency vibrations can be beneficial to the human body, as all body does vibrate at a certain frequency. Zhao, Bo, et al. [33] found an inverse correlation between static load and ultrasonic amplitude in ultrasonic machining. With an increase in static load, there is a decrease in ultrasonic amplitude after an initial rise occurs. Various studies of vibration

have been conducted throughout the years in various areas, such as human anatomy, civil and structural engineering, mechanics, automotive industry, etc.

Most vibration studies conducted for the automotive industry have been on brake disc and these have mainly been squeal analysis and brake judder analysis. Brake judder is a braking induced forced vibration occurring in different types of vehicles. Brake judder is usually felt in the steering wheel, which affects the operation of the vehicle and can cause veering. Hence, the study of such has been prudent so as to reduce the transfer frequency from the brake to the steering wheel. Squeal is defined as a noise that occurs when a system experiences very high amplitude mechanical vibrations. Brake squeal typically is either a low frequency vibration or a high frequency vibration usually caused by worn out pads and other conditions. Although, certain low frequency vibrations have been introduced to the human body for scientific purposes, Jr, M. Triches, et al. [40] stated that typically, the high frequency squeal occurs for frequency ranges between 8 and 16 kHz, while low frequency squeal occurs between 1 and 7 kHz, but since the human ear is most sensitive to the frequency region between 1 and 4 kHz, the low frequency squeal is considered the most annoying type of brake noise. Nishiwaki [29] studied the dependency of disc brake squeal on the natural frequency of cantilever type pad-caliper, which occurred at 2.7 kHz, 2.0 kHz and 5.3 kHz for each cantilever length L=40 mm, 50 mm and 80 mm in each friction test. Kumemura [28] deduced that the phenomenon of low frequency squeal of disc brake occurs only under special conditions and the occurrence rate is very small compared to high frequency squeal. Jr, M. Triches, et al. [40] also stated that low frequency disc brake noise is a problem that typically occurs in the frequency

range between 100 and 1000 Hz and typical examples of noise problems from this category are groan and moan noises. Also, the generation mechanism of this kind of problem is the friction excitation at the rotor and lining material, which provides energy to the system. This energy is transmitted as a vibratory response through the brake assembly and couples with components of the suspension and chassis. Hu, Shugen, and Yucheng Liu [36] concluded in a research that the probability of brake noise generation increases with the increasing brake pressure because the velocity feedback causes a negative equivalent damping, which increases with the increasing brake pressure, and the probability of brake noise generation increases with the decreasing disc rotational speed because the slope of the curve decreases with the decreasing disc rotational speed, and the negative equivalent damping caused by the velocity feedback decreases as the speed decreases, which also decreases the total system damping. Duan, C, and R Singh [39] found that peak vibration levels of the steering wheel were seen when the rotational frequency of the tire coincided with the resonant frequency of the transfer path. They proposed a new vibration control concept that modulates the actuation pressure. The concept they proposed is based on an approximate solution for the angular displacement of the disc in the model they developed. Their preliminary work also indicated that the concept could be very effective in reducing the receiver vibration level without sacrificing the brake performance. Hajnayeb, Ali, et al. [42] found in their study of brake judder that the first two modes of the wheel are the dominant vibration modes and the vibration signal of the brake pedal has similar components to the steering wheel, except for showing lower vibration amplitudes in the natural frequencies of the transfer path.

Meyer, Ralf [41] studied disc brake judder that is attributable to thickness variations in the disc and that these deviations from the ideal plane surface can be caused either by wear and corrosion or by thermal stresses (changes within the microstructure of the disc material). They are termed “cold judder” and “thermal judder” respectively. This thesis studies vibration due to rotation of the tires, the vibration observed in this study has components of deflection in the axial, radial, and circumferential direction but with the majority of its deflection in the axial direction. This vibration study was used in a coupling analysis with thermal buckling to study the effects of vibration on thermal buckling and thermal buckling temperature on vibration.

2.2 Review of Thermal Buckling Study

It is well known that automotive brakes and clutches can fail at elevated temperatures and thermal stresses due to the frictional heat generation at the contact surfaces during brake operations or clutch engagements. The mechanism of failure, however, varies depending on the operating conditions. Timošenko Stepan Prokofʹevič, and James Monroe Gere [7] published the most important failure mechanisms include thermoelastic instability or hot spotting, thermal cracks and thermal buckling and among them, thermal buckling is believed to be one of the dominant failure mechanisms in clutch plates due to their small thicknesses. Instability problem was first observed by Euler Bernoulli. Euler’s method was revised and now used today to tackle buckling loads in linear elastic problems. Bigoni, D., et al.[31] showed that the sliding movement of the end of a structure against the curvature of the constraint strongly affects buckling loads.

Buckling is a widespread phenomenon that have been studied at various disciplines of engineering and for various geometries. Ari-Gur, Judah, and Samuel R. Simonetta [32] found that dynamic buckling can occur for lower loads at a range of loading frequencies near the fundamental frequency of a plate. They also found axial displacement in buckling is not sensitive to material configurations. Pegg, N.g.[34] discovered that buckling failure during dynamic response is shown to occur at peak loads that are much higher, and in modes which consist of much smaller wavelengths than static buckling loads. The buckling mode shape also changes significantly during its formation due to the effects of strain rate and curvature reversal. Stibich, Paul R., et al. [34] published a technique to predict thermal buckling in automotive body panels, by obtaining vehicle body temperature profile from a heat transfer analysis and is applied in the buckling analysis.

The research of thermal buckling is important in both mechanical and material engineering, particularly in automotive systems to study and simulate realistic applications. Audebert et al. [38] studied buckling of automotive clutch plates due to thermoelastic residual stresses. It was based on a tent-like temperature distribution, which was all theoretical. The results showed that clutch plates subjected to axisymmetric temperature excursions can develop residual in-plane bending moments of sufficient magnitude to cause buckling during unloading. The coning mode occurred when the residual stress at the outer radius was tensile and the potato chip mode occurred when it was compressive. Ma [13] extended the method to automotive disk brakes and investigated the effect of geometric and material parameters on the critical buckling loads via the

finite element method. These studies revealed that both axisymmetric and non-axisymmetric buckling modes can be caused by a uniformly distributed thermal loading in the circumferential direction. In addition, a slightly changed temperature profile in the radius can greatly affect the deformed shape of the buckling mode.

In this chapter, the studies on vibration, mechanical buckling, and thermal buckling have been reviewed. In previous studies, various methods have been used to analyze vibrations and buckling. Various geometries have been considered in both studies. In vibration studies geometries such as rectangular plates and in thermal buckling geometries such as plates, beams, etc. Vibration studies conducted or analyzed in automotive brake disc have been noise or squeal analysis. Thermal buckling studies analyzed in brake disc have all been simplified to annular rings or hat section. The present work will incorporate the theory of thermal buckling first introduced by Euler and the governing eigenvalue problem of buckling to investigate the coupling of vibration and thermal buckling in brakes by taking into account various vehicle speeds that affect the vibration modes and in turn affect the buckling temperature. The vibration study is based on a forced vibration due to tire rotation at various speeds of the vehicle. A more realistic model of a brake rotor will be the model analyzed in this study. Based on previous works, finite element analysis has proven to be efficient in analyzing vibrations and thermal buckling. Therefore, finite element analysis is chosen for the coupling numerical study of vibration and thermal buckling in automotive brake discs.

CHAPTER THREE: FINITE ELEMENT MODEL AND SETUP

Finite element analysis is a numerical method for solving physics and mathematical problems. Finite element analysis is used to solve real-world problems that cannot be easily solved using analytical solutions. Most problems are generally complex, so, when using numerical methods the problems are simplified to get an accurate understanding of the problem. Due to these reasons finite element method was used in this thesis. Palmer, E, et al. [43] stated in high-demand braking applications, vented discs are increasingly being used as these are considered to have high heat-dissipating characteristics. Therefore, a vented brake rotor is the chosen model for the purpose of the analysis of this thesis. The geometric model of the brake rotor is based on the benchmark brake model for squeal analysis in ABAQUS [5] which was then modified and simplified not to include the brake pads. Maluf, Omar et al. [14] published that cast irons are commonly used in brake discs production, the low costs of the production, the excellent thermal conductivity, the ease of dissipating heat generated by the friction of the pads during a stop, and the capacity of damping vibrations, which are prime characteristics of this kind of component. Therefore, cast iron was the chosen material for this study.

The 3D model is composed of tetrahedron element type with 34,984 nodes and 19,116 elements. Figure 3-1 shows the modified brake rotor in the meshed state before the analysis is conducted. Table 3-1 shows dimensions for the brake rotor and Table 3-2

shows the material properties for gray cast iron. Figure 3-1 shows the side view and top view of the brake rotor to illustrate the dimensions shown in Table 3-1. The setup for the study only required some constraints be placed on the model. The constraints on the model followed a realistic boundary condition for a brake rotor, where the brake rotor is fixed to the wheel of the car via the bolts, and the inner and outer radii are free. A fully fixed constraint was placed on the bolt holes in the disc rotor. The constraint used was the same for the vibration simulation, thermal buckling simulation, and coupling simulation. The vibration study was given an initial condition of rotational velocity; the rotational velocity was applied in the circumferential (theta) direction. The loading condition for the thermal buckling simulation is a temperature gradient distributed in either the radial, axial or circumferential direction. Generally, to realistically characterize the coupling study, the type of vibration that occurs is a forced vibration; it is a forced vibration due to the rotating speed of the wheel of the vehicle.

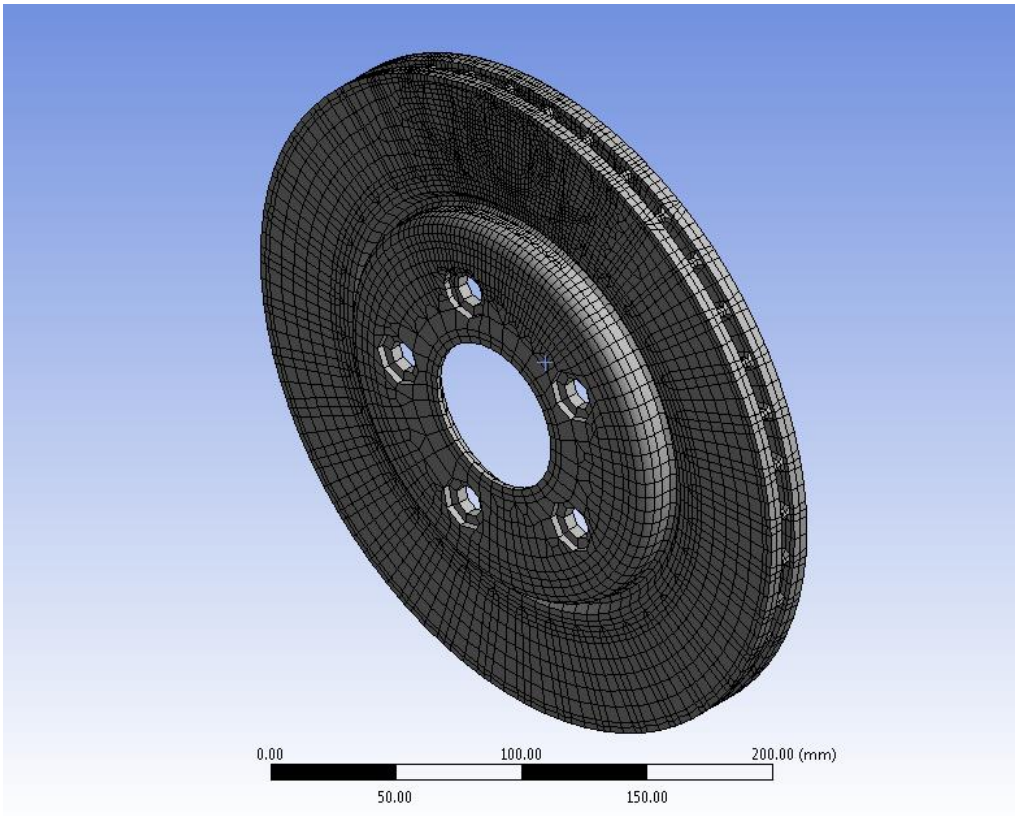

Figure 3-1**:** Finite Element Model of a Brake Rotor [5]

Table 3-1: Geometric Dimensions of the Brake Rotor

	Outer Radius	Inner Radius	Hat Diameter	Hat Height	Thickness
Symbol	Ro	Ri	Dh	Hh	t
Unit	mm	mm	mm	mm	mm
Value	144	32	184	13	20

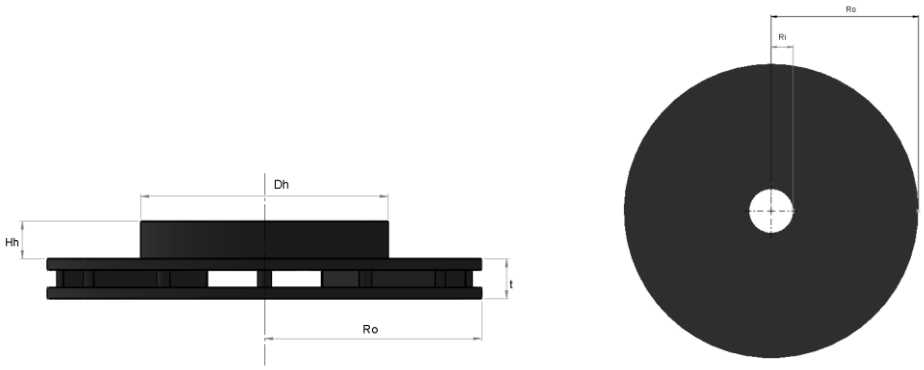

(a) (b)

Figure 3-2: Brake rotor dimension illustration

Table 3-2: Material Properties of the brake rotor

	Young's Modulus	Mass Density	Poisson's Ratio	Thermal Expansion	Thermal Conductivity	Specific Heat
Symbol	E	ρ	ν	α	k	Cp
Unit	Pa	N/m		10-6/K	W/m*k	J/kg*k
Value	6.6178x1010	7200	0.27	12	45	510

ABAQUS proved to have a longer run time, and occasionally did not yield any results for the proposed simulation later on in this thesis. So, the model used was obtained from ABAQUS benchmark and the simulations were conducted on ANSYS. The ABAQUS input file with the node coordinates and element number was modified to eliminate the brake pads and backer plates for both the vibration and thermal buckling simulations. All simulations were run using the graphic user interface in ANSYS workbench. The input file was saved in its original format of .inp and imported into ANSYS using the finite element modeler tool from the ANSYS toolbox. The vibration

simulation was run using the modal analysis system. The modal analysis system was linked to the finite element modeler and used as the model for simulation. In the modal analysis system the engineering data can be modified, the material properties for gray cast iron were added to the material data library to be used in both analyses. The model was opened in ANSYS mechanical from the modal analysis system in ANSYS workbench. Here the model was meshed, and the default mesh created had 34,984 nodes and 19,116 elements. A convergence study was conducted by creating a mesh control varying the element size. The element sizes are measured in mm, and changed from default to 20mm, 15mm, 10mm, and 5mm, the smaller the element size the larger the number of nodes and elements. A mesh behavior of hard was chosen instead of the default soft, because the hard behavior keeps the prescribed element size settings and number of divisions for the edges, unlike the soft behavior which can cause the mesh control to be affected by the curvature and often results in a different number of nodes and elements every time the model is remeshed. A new coordinate system was created specifically for loading conditions, and a more preferred cylindrical coordinate was chosen and created for a disc. The coordinate system was created to be able to accurately obtain the radial, axial and circumferential deformation results. Fixed supports were applied to the model at the bolt holes from the supports menu, and a rotational velocity was introduced from the inertial menu and the vibrational simulation was run and the deformations obtained. The deformation result was obtained by exporting the deformation result from ANSYS Mechanical Analysis Module after the simulation had concluded.

The thermal buckling analysis had a similar setup to the vibration analysis in ANSYS workbench, but instead of a modal analysis system, it was a multistage setup. First a static analysis system was linked to the finite element modeler model and a linear buckling analysis system was linked to the model, setup and solutions tabs in the static analysis system. Similar fixed supports were used in the thermal buckling analysis, the same cylindrical coordinate system was created for the model in ANSYS Mechanical, and the thermal load was applied in the static study which transferred to the linear buckling study. The thermal loads were applied to the model using the newly created cylindrical coordinate and not the global cartesian coordinate. The setup for the thermal buckling was concluded and the simulation was run.

CHAPTER FOUR: VIBRATION ANALYSIS

Rotating machinery produces vibration during its normal operation as a consequence of friction and centrifugal forces of both the rotating parts and the bearings. As a result, vibration can be measured, recorded, trended, and in most cases even heard. Thus, we define vibration as a repetitive movement around a point of equilibrium characterized by its variation in amplitude and frequency [6].

A type of vibration in a brake disc is brake judder. Brake judder can usually be noticed during braking because, the contact surface between the brake rotor and brake pads changes. This changing contact surface can be caused by different various phenomena such as warped rotor, material defect, unaligned rotor and TEI (thermoelastic instability), just to name a few. Vibration can also affect the heat dissipation process during braking, and this can lead to rapidly increasing and very high temperatures in the brake disc. It is also known and shown in Tables 4-1, 4-2 and 4-3 that at low traveling speeds the vibration of the brake disc can be high and at higher speeds the vibration reduces.

Using the modal studies in ANSYS a vibration analysis was performed to find the vibration modes of the brake rotor's frequencies. The simulation for vibration was setup with fixed supports at the bolt holes and given an initial condition of rotational velocity. The rotational velocity was obtained and calculated using Equation 1, assuming a

traveling speed of the vehicle in miles per hour (mph). The linear speed of the vehicle in miles per hour (mph) was converted to meters per hour, then using the circumference of the wheel in meters convert meters per minute to revolutions per minute (rpm), which was finally converted to rotational velocity in radians per second (rad/s).

$$RV = S_v * \frac{1609}{3600r} \quad (1)$$

Here RV represents rotational velocity in radians per second, S_v represents speed of vehicle in miles per hour and r represents the radius of the wheel in meters, not to be confused with the radius of the brake rotor. The radius of the wheel used in this study is based off Daws, J. W., et al [20] Chevrolet Avalanche wheel radius of 778mm (0.778m). The study was conducted at three various vehicle speeds with a low speed of 25mph (generally a school zone maximum speed limit), a high speed of 75mph (generally a highway maximum speed limit) and a highway minimum speed limit of 55mph. Using Equation 1, the calculated rotational velocities from the speeds of 25mph, 55mph, and 75mph are 14rad/s, 32rad/s and 43rad/s respectively. Tables 4-1, 4-2 and 4-3 show the convergence study by varying the element size, obtaining the number of nodes and element, computing the vibration frequency and calculating the percent error between the computed frequencies to determine the best element size for an accurate result. A chosen medium mesh density was used. The medium mesh density is half way between a fine mesh density and a coarse mesh density.

Table 4-1: Convergence study for a rotational velocity of 14rad/s

Tetrahedron Element Type				
Vehicle Speed of 25 MPH				
Element Size [mm]	Number of Nodes	Number of Elements	Frequency [Hz]	Percent Error [%]
Default	34984	19116	769.96	
20	16053	8143	798.54	3.579031733
15	19826	10143	785.52	1.657500764
10	31651	16601	773.31	1.57892695
5	105806	61366	751.18	2.946031577

Table 4-2: Convergence study for a rotational velocity of 32rad/s

Tetrahedron Element Type				
Vehicle Speed of 55 MPH				
Element Size [mm]	Number of Nodes	Number of Elements	Frequency [Hz]	Percent Error [%]
Default	34984	19116	767.46	
20	16053	8143	796.72	3.672557486
15	19826	10143	783.03	1.74833659
10	31651	16601	770.78	1.589299152
5	105806	61366	748.62	2.960113275

Table 4-3: Convergence study for a rotational velocity of 43rad/s

Tetrahedron Element Type				
Vehicle Speed of 75 MPH				
Element Size [mm]	Number of Nodes	Number of Elements	Frequency [Hz]	Percent Error [%]
Default	34984	19116	765.89	
20	16053	8143	795.36	3.705240394
15	19299	9760	781.47	1.777419479
10	31651	16601	769.21	1.593843034
5	105806	61366	747.04	2.967712572

Figure 4-1 is the deformed result of the first mode vibration with a rotational vibration 32rad/s and an element size of 10mm, with a result frequency of 770.78 Hz. It also shows a color spectrum from blue to red; blue being the smallest deflection of 0mm and red being the maximum deflection of 20.992mm. The deformation shown in Figure 4-1 is the total deformation of the brake rotor in mm. Figure 4-2a&b below shows the potato chip mode and coning mode deformations in millimeters (mm) corresponding to the third and ninth mode respectively at 55mph and 10mm element size, with maximum deformation of 23.553mm and 24.799mm, respectively. The third and ninth modes are the first potato chip and coning modes observed at 55mph; this also holds true for both speeds of 25mph and 75mph. At a speed of 55mph the frequencies corresponding to modes 3 and 9 are 1069.4 Hz and 3715.3 Hz respectively.

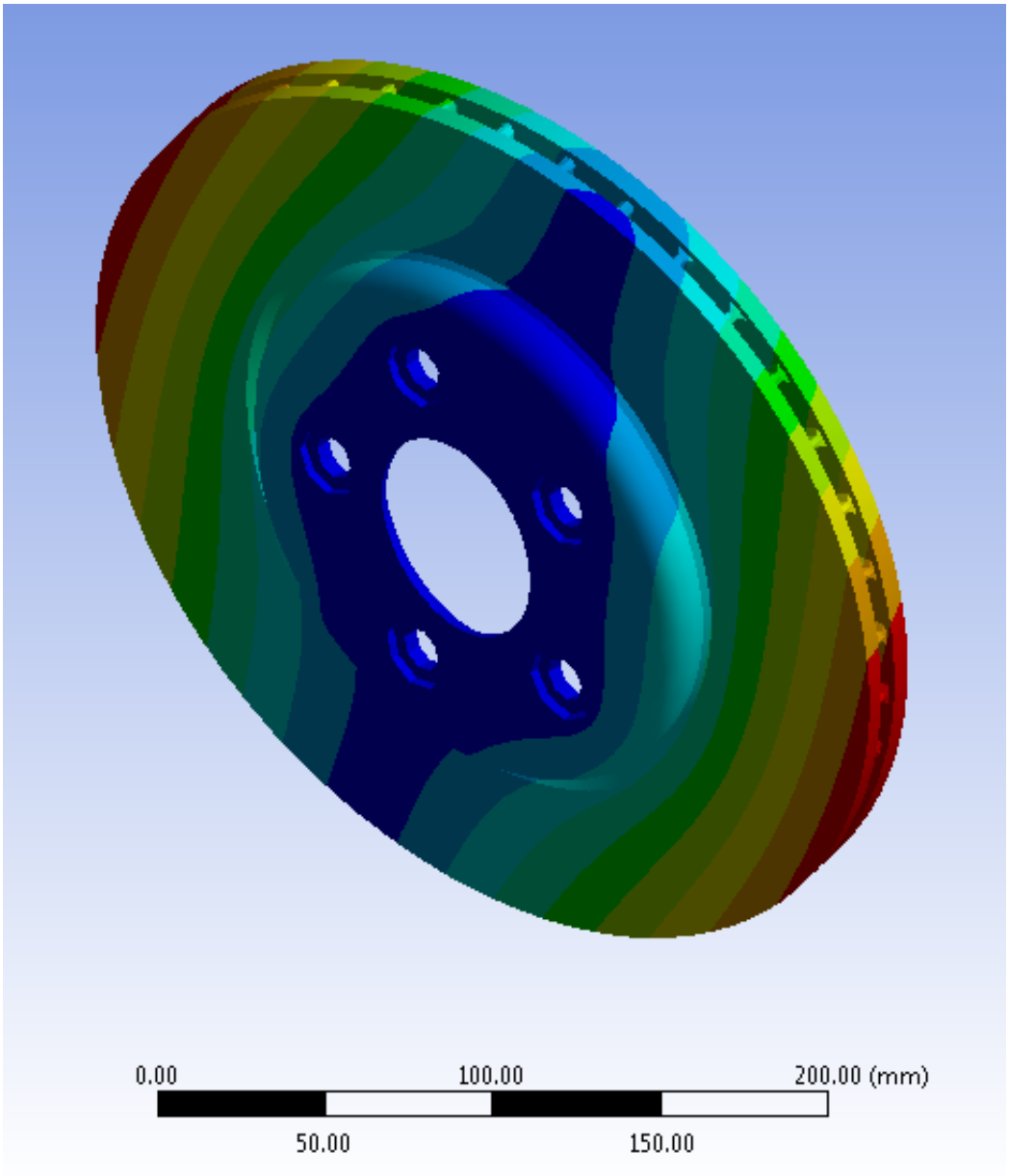

Figure 4-1**:** Mode 1 (dominant mode) total deformation in mm of the brake rotor

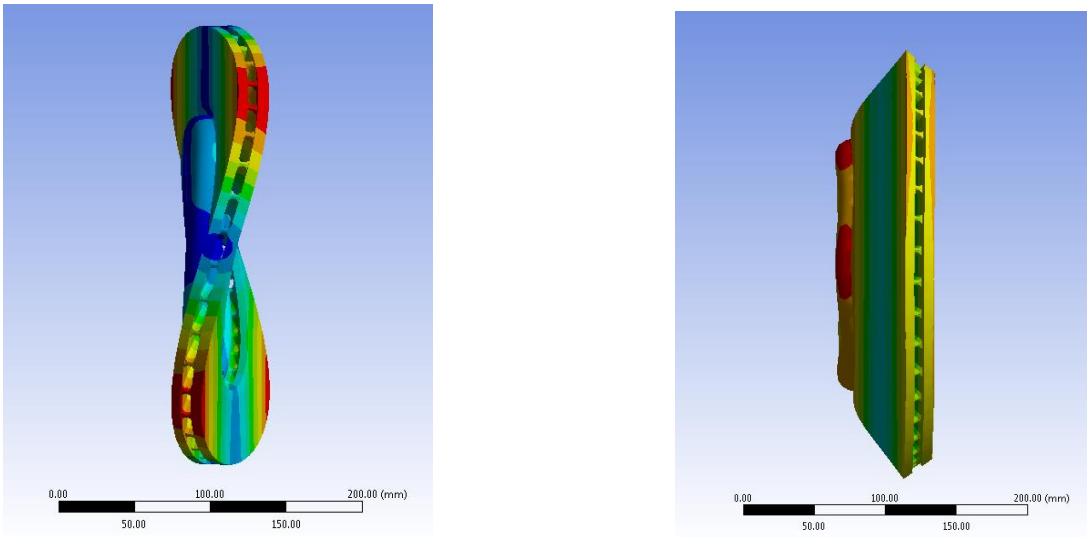

(a) (b)

Figure 4-2: Deformation in mm with an initial rotational velocity of 32rad/s: (a) mode 3: potato chip mode; (b) mode 9: coning mode.

It should be noted that the deformation obtained from this vibration analysis will be used in Chapter 6 the coupling of vibration and thermal buckling study. It is also prudent to look at the radial, axial and circumferential deformation. The potato chip and coning modes remain the same as modes 3 and 9 respectively for all the directional (radial, axial and circumferential) deformation. Figures 4-3, 4-4 and 4-5 show the first mode deformation in the radial, the axial and the circumferential direction in mm respectively with a rotational velocity of 32rad/s. The color spectrum observed in all the figures in this chapter denotes blue as the minimum deflection and red as the maximum deflection. The maximum and minimum deflection in Figure 4-3 is 5.2648mm and -5.2522mm respectively and for Figures 4-4 and 4-5 the corresponding maximum and minimum deflections are 20.353mm and -20.296mm; 4.0692mm and -4.0244mm

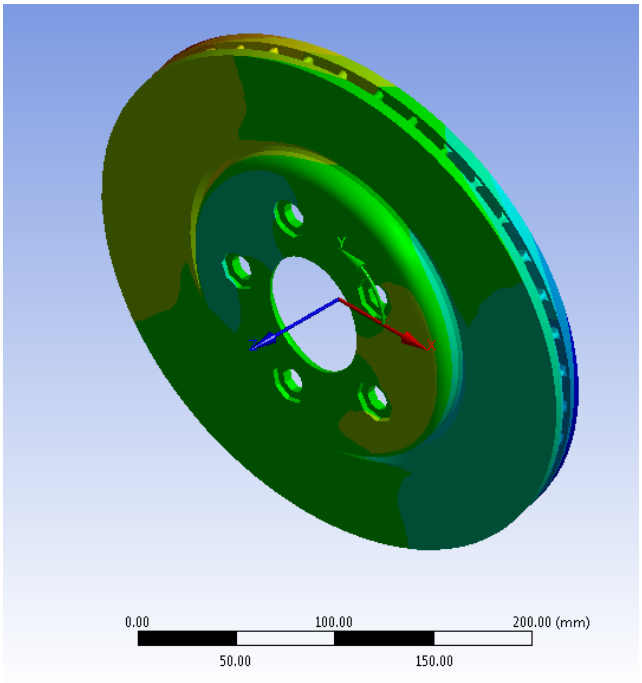

Figure 4-3: Mode 1 radial (X) deformation in mm with 32rad/s rotational velocity

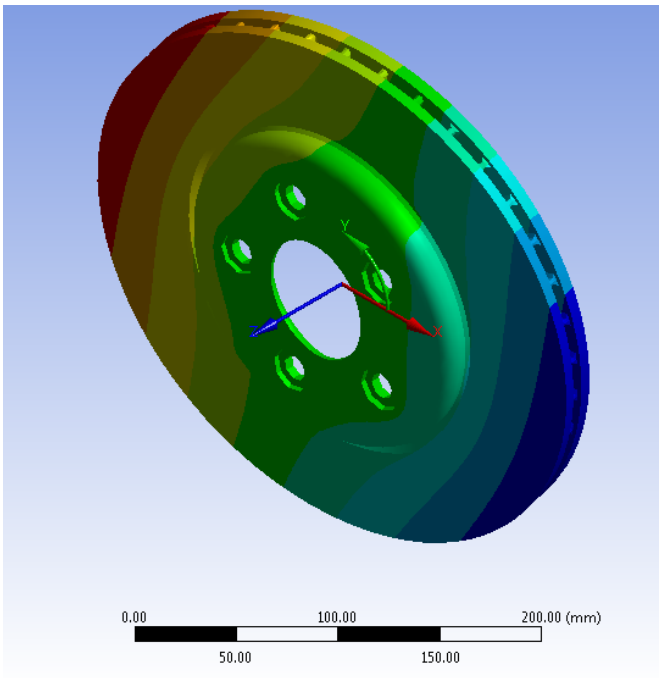

Figure 4-4: Mode 1 axial (Z) deformation in mm with 32rad/s rotational velocity

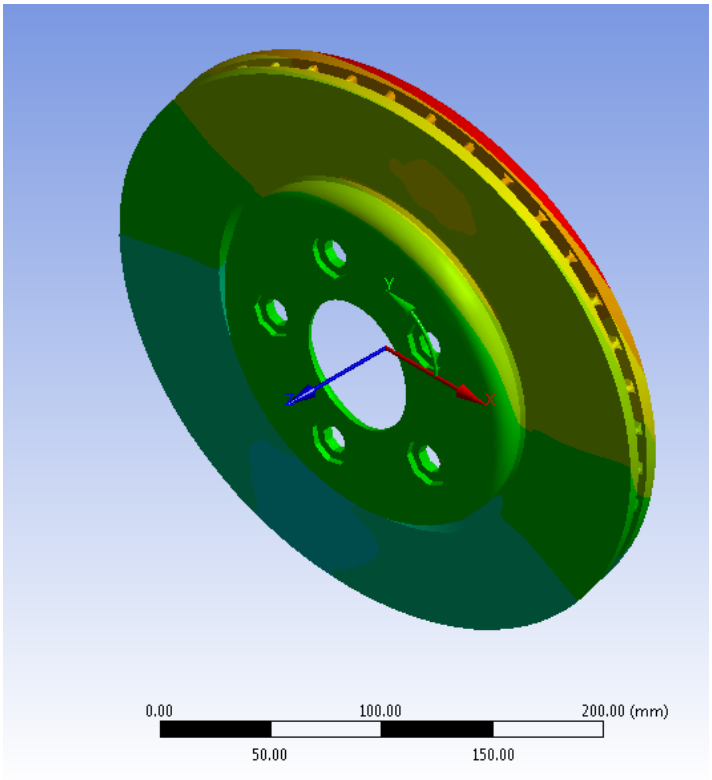

Figure 4-5: Mode 1 circumferential (Y) deformation in mm with 32rad/s rotational velocity

The total deformation of the brake rotor for mode 1 obtained from the vibration simulation with an initial rotational vibration of 32rad/s has a frequency of 770.78Hz and a maximum deflection at approximately 22mm and the minimum deflection at 0mm. Figures 4-6 and 4-7 show mode 1 plot of the radial deformation vs the radial location and the axial deformation vs the axial location with a 32rad/s rotational velocity. The plots show the profile of the deformation, Figure 4-6 shows a profile that looks like the plot of a cube root (x^3) function. The plots will be used in Chapter 6 to calculate and construct a temperature profile that matches the deformation profile. Figures 4-7 and 4-8 show a plot

of the radial and axial deformation as a function of radial location on the midplane of the thickness.

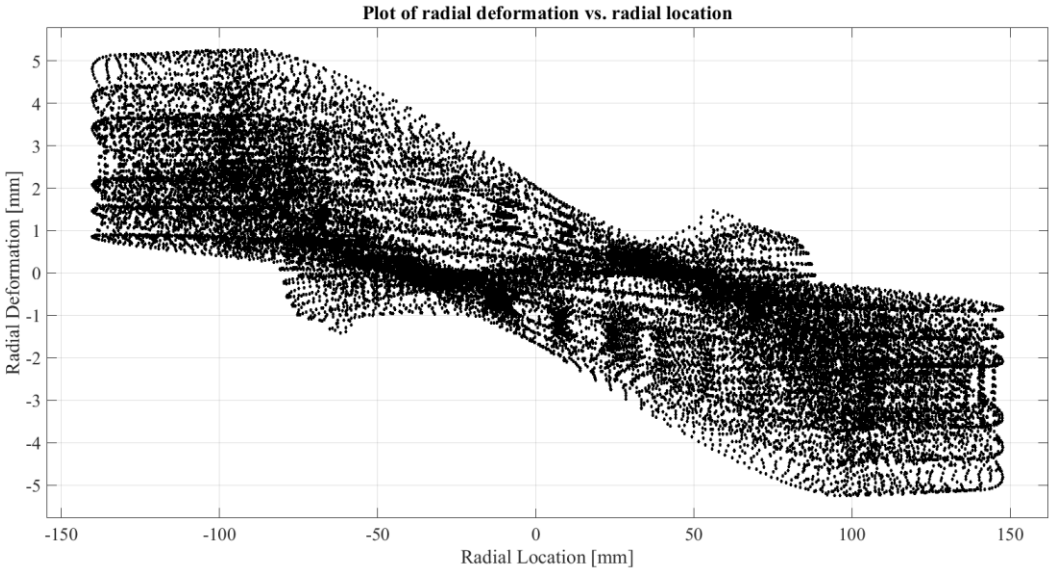

Figure 4-6: Plot of radial deformation vs. radial location

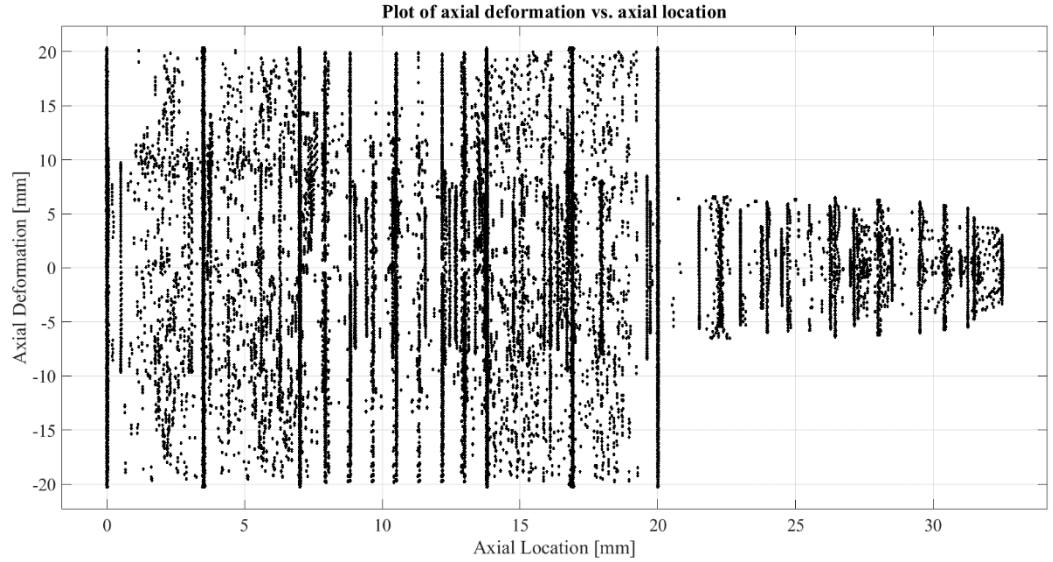

Figure 4-7: Plot of axial deformation vs. axial location

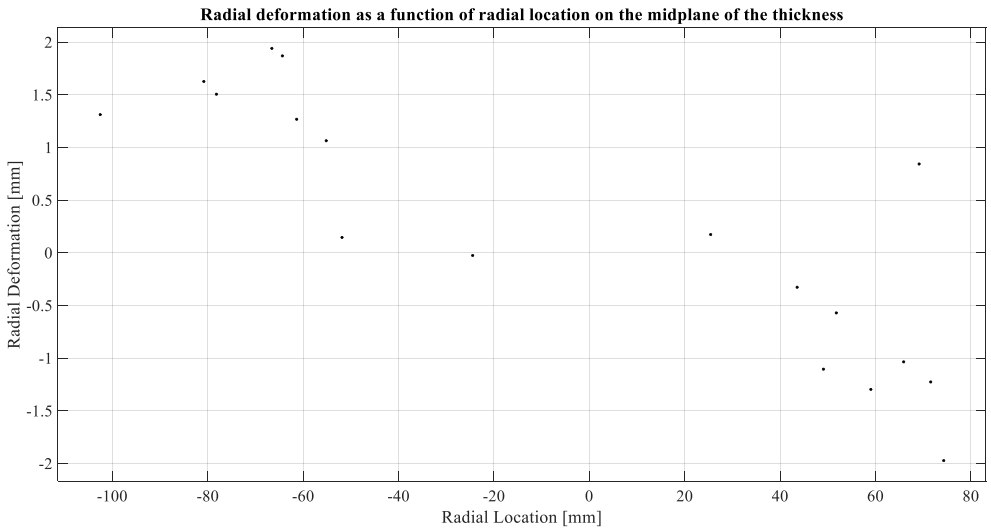

Figure 4-8: Radial deformation vs. radial location on the midplane of the thickness

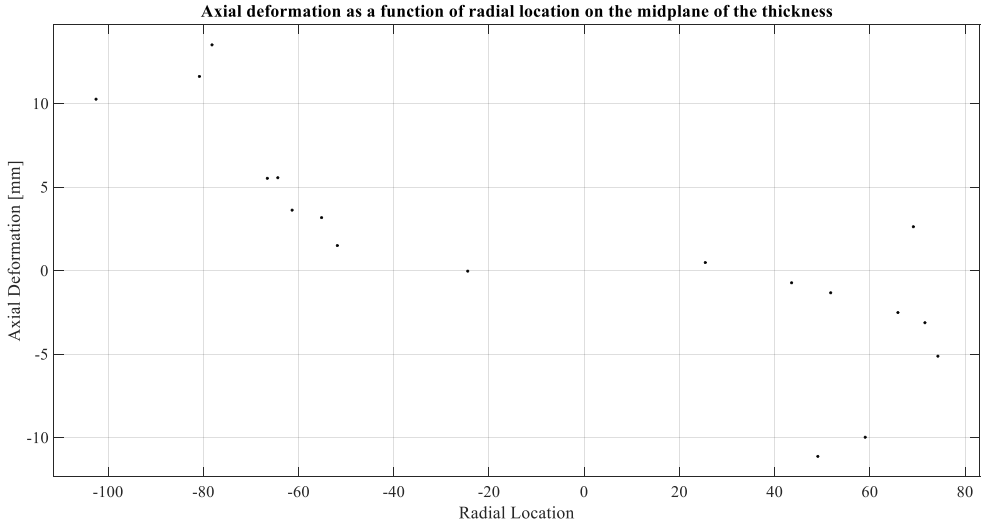

Figure 4-9: Axial deformation vs. radial location on the midplane of the thickness

CHAPTER FIVE: THERMAL BUCKLING ANALYSIS

5.1 Thermal buckling overview and effect of radial temperature distribution

When the brake is applied, the pistons in the caliper are engaged and push the friction pads which in turn apply pressure to the brake rotor. This creates friction between the brake pads and brake rotor, and this friction generates heat and creates a distribution of temperature along the radial direction in the brake rotor. The temperature distribution in turn causes a phenomenon known as thermal buckling. Thermal buckling occurs when a non-uniform temperature is applied to a body. Zhao, Jiaxin, et al. [8] stated that automotive transmission clutches and brakes undergo different operating conditions, such as the initial engagement, full contact and plate separation stages. As a result, various temperature distributions in the clutch plates and brake rotor are possible. Linear, exponential and sinusoidal distributions have been found among the most representative temperature profiles. The linear distribution can be caused by the sliding speed as a linear function of the radius and by the fact that the frictional heat generation rate is a linear function of the sliding speed. The sinusoidal distribution is related to the local high-temperature regions known as hot spots that could be excited by thermoelastic instability. An exponential distribution can be caused by the non-uniform convective cooling on the surface or a non-uniform contact pressure during the engagement and separation of plates and similarly the engagement and separation of the rotor and brake pads. For the reasons

stated by Zhao, Jiaxin, et al. [8], this study assumed a linear temperature profile, a sinusoidal temperature profile and an exponential temperature profile distributed in the radial direction. In the first scenario, the temperature distribution in the axial direction (thickness) is uniform. Because, the distribution in the axial direction is negligible compared to the temperature distribution in the radial direction. Likewise, in the second scenario the temperature is distributed in the axial direction, and uniform in the radial direction.

The below equation is the governing equation for the eigenvalue problem of buckling.

$$\left([K] + \lambda_{cr}[K_\sigma]_{ref}\right)\{\delta D\} = \{0\} \tag{2}$$

Here the term "*ref*" represents the reference load, i.e., a load that is first applied to the structure to find the reference stress stiffness matrix, $[K_\sigma]_{ref}$. Another load $\{R\} = \lambda_{cr}\{R\}_{ref}$ will then be applied to the structure, where λ_{cr} represents an arbitrary multiplier to the original reference load. The critical buckling load in a buckling analysis under mechanical or thermal loading is the product of the applied reference load and the calculated critical buckling eigenvalues. The most important buckling deformation mode is the mode with the lowest critical buckling temperature. The temperature distributions in the analysis are set as increasing from the inner radii to the outer radii of the rotor following either a linear, sinusoidal or exponential pattern, meanwhile having the inner and outer radii free to move but constrained at the bolt holes.

Based on Timoshenko's [13] beam theory, the critical bending moment that causes the buckling of a disc can be determined by the following equations.

$$K = \frac{1+\nu}{2};\ a = R_b - R_a;\ R = \frac{R_a+R_b}{2}; \tag{3}$$

$$M = \frac{1+K}{2} \pm \sqrt{\left(\frac{1-K}{2}\right)^2 + Kn^2} \tag{4}$$

In the above equations, K, ν, M, n, E, t, R_a and R_b represent the stiffness ratio, Poisson's ratio, the dimensionless critical bending moment, the buckling wave number, Young's modulus, the disc thickness, the inner radius, and the outer radius, respectively. When n=0, the two calculated values of M are 1 and 0.65. The smaller value of M should be used to calculate the critical bending moment.

The bending moment caused by the thermal stress in an annular ring can be obtained through the following equation.

$$M_b = \int_{R_a}^{R_b} t\sigma_{\theta\theta}(r)(r-R)dr \tag{5}$$

When the inner and the outer radii are free, $\sigma_{\theta\theta}$ can be expressed as

$$\sigma_{\theta\theta}(r) = \frac{\alpha E}{r^2}\int_{R_a}^{r} rT(r)dr - \alpha ET(r) + \frac{EC_1}{1-\nu} + \frac{EC_2}{(1+\nu)r^2} \tag{6}$$

$$C_1 = \frac{\alpha}{2(1-\nu)}\frac{1}{R_b^2-R_a^2}\int_{R_a}^{R_b} rT(r)dr \tag{7}$$

$$C_2 = \frac{\alpha(1+\nu)R_a^2}{R_b^2-R_a^2}\int_{R_a}^{R_b} rT(r)dr \tag{8}$$

$$T(r) = \frac{\Delta T}{R_b - R_a}(r - R_a);\ \Delta T = T_b - T_a \quad (9)$$

where α, $T(r)$ and ΔT represents the coefficient of thermal expansion, the temperature distribution along the radial direction and the temperature difference between the outer and inner radii, respectively. The critical buckling temperature is defined as the product of the highest nodal temperature and the computed load multiplier. Having the bolt holes fixed in all three directions, the dominant buckling deformation mode has a wavy shape that looks like a potato chip with a load multiplier of 46.426. The corresponding critical buckling temperature is 1.1607×10^4 ºC, which can be considered as the upper bound of the result. Here the load multiplier is known as the eigenvalue. The eigenvalue can also be considered and the buckling load factor, the buckling load factor is the number obtained from the simulation that determines the lowest acceptable load before buckling occurs, in this case, the lowest acceptable temperature before buckling occurs. The lowest acceptable temperature is also the critical buckling temperature.

It can be noted that the range of temperature variation (i.e. the difference between the highest temperature and the lowest temperature) increases with the coefficient of friction. The eigenvalues increase with the ranges of temperature variations in the radial direction. The profile of temperature distribution can significantly affect the critical buckling temperature and the associated buckling deformation mode.

Figure 5-1 shows the temperature profile obtained using the linear equation shown in Table 5-1 and dimensions shown previously in Table 1-1. Figure 5-2 shows the

first mode deformation for the thermal buckling analysis. The first mode being the dominant mode with load multiplier used to calculate the critical buckling temperature. The deformed first mode of the brake rotor with a linear temperature profile distributed in the radial direction is known as the potato chip mode because its deformed shape looks like that of a potato chip. Figure 5-3 shows the deformed thermal buckling mode of the second mode with a linear temperature profile distributed in the radial direction; the second mode also known as the coning mode, because the deformed shape looks like a cone. All deformations in this thermal buckling analysis are axial (thickness direction) deformation. The equations and constants are chosen such that the temperature difference for each scenario is the same at 228°C across the radius, with a low and high of 22°C at the inner radius and 250°C at the outer radius respectively. The blue color in the figures indicates the low temperature and the red indicates the high temperature. Modes 1 and 2 deformations of the thermal buckling analysis with the given temperature profiles below distributed along the radial direction are the potato chip mode deformation and coning mode deformation.

Table 5-1: Assumed temperature profile in the radial direction

Temperature Profile	Equation	Load Multiplier	Critical Buckling Temperature
Linear	$228 * \left(\frac{r-32}{144-32}\right) + 22$	46.426	1.1607×10^4 °C
Sinusoidal	$228 * \sin\left(0.80357 * (r-32)\right) + 22$	61.861	1.5465×10^4 °C
Exponential	$228 * [\frac{\exp(0.2222 * (r-32)) - 1}{573.8629 \times 10^6 * (144-32)}] + 22$	68.393	1.7098×10^4 °C

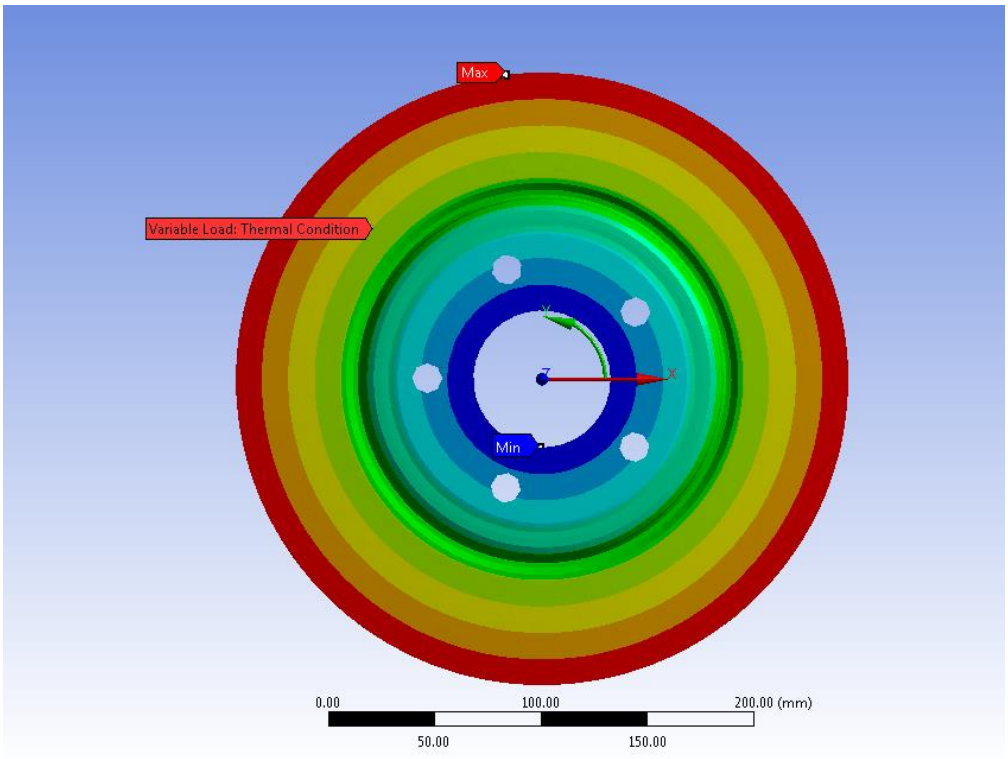

Figure 5-1**:** Linear temperature profile in the radial direction

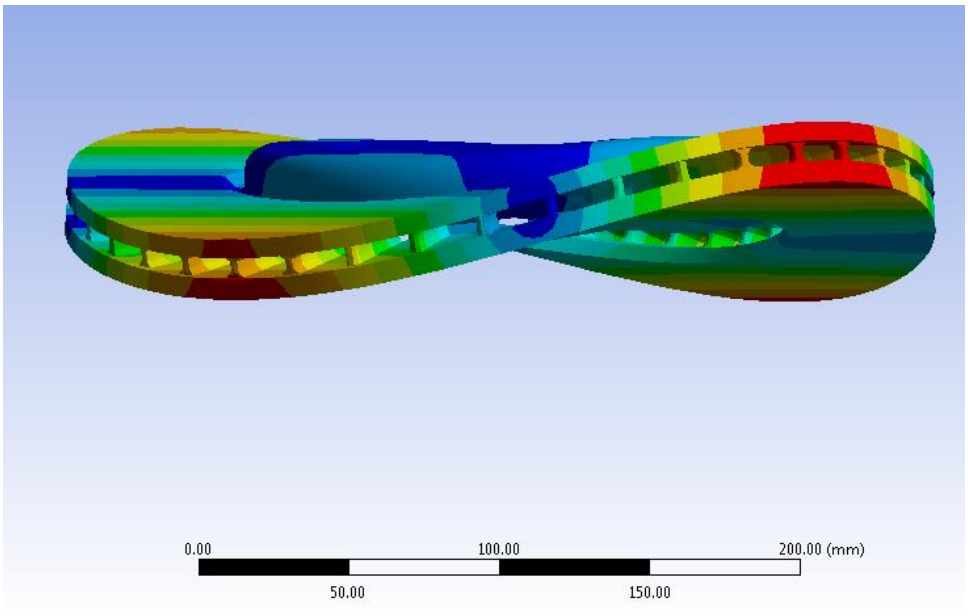

Figure 5-2: Mode 1 potato chip deformation in mm with above linear temperature profile.

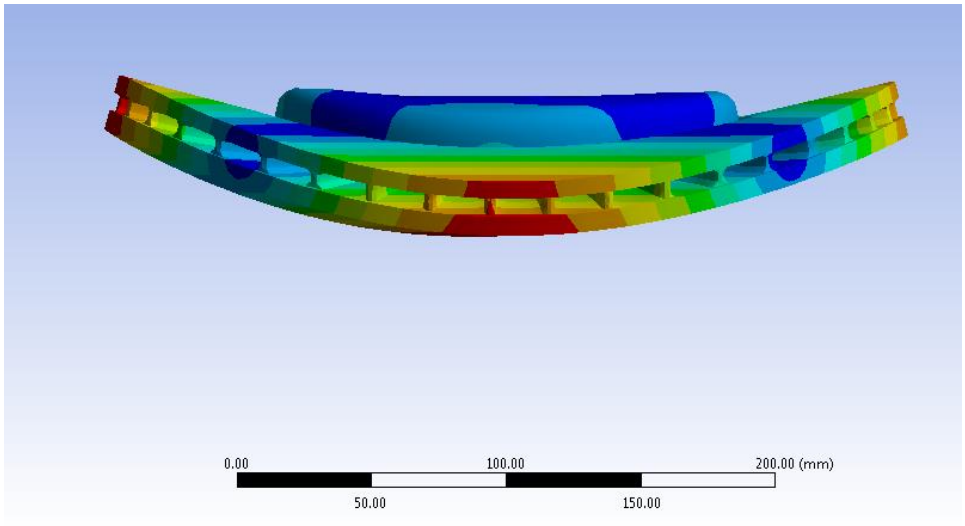

Figure 5-3: Mode 2 Coning mode deformation in mm with above linear temperature profile.

5.2 Effect of axial (thickness) temperature distribution

In the previous analysis in Section 5.1, the temperature distribution was applied in the radial direction and the temperature in the thickness direction was considered uniform. In this analysis the temperature is varied in the thickness direction and uniform in the radial direction. This study is to find the effect of having a variable temperature in the thickness direction and how it compares to having a radial variable temperature. Figure 5-4 shows the axial temperature distribution. The critical buckling temperature with the axial variable temperature distribution is 5.2972×10^4 °C. Unlike the radial temperature distribution having both the potato chip and coning modes as modes 1 and 2 respectively, the potato chip and coning modes are modes 6 and 7 respectively for an axial temperature distribution with a linear profile. The temperature varies from the hat head to the bottom of the rotor. The hat head showing a blue color denotes the lowest temperature and the red color on the bottom of the rotor denotes the highest temperature. Also, in this simulation, it is good to note the circumferential temperature is uniform.

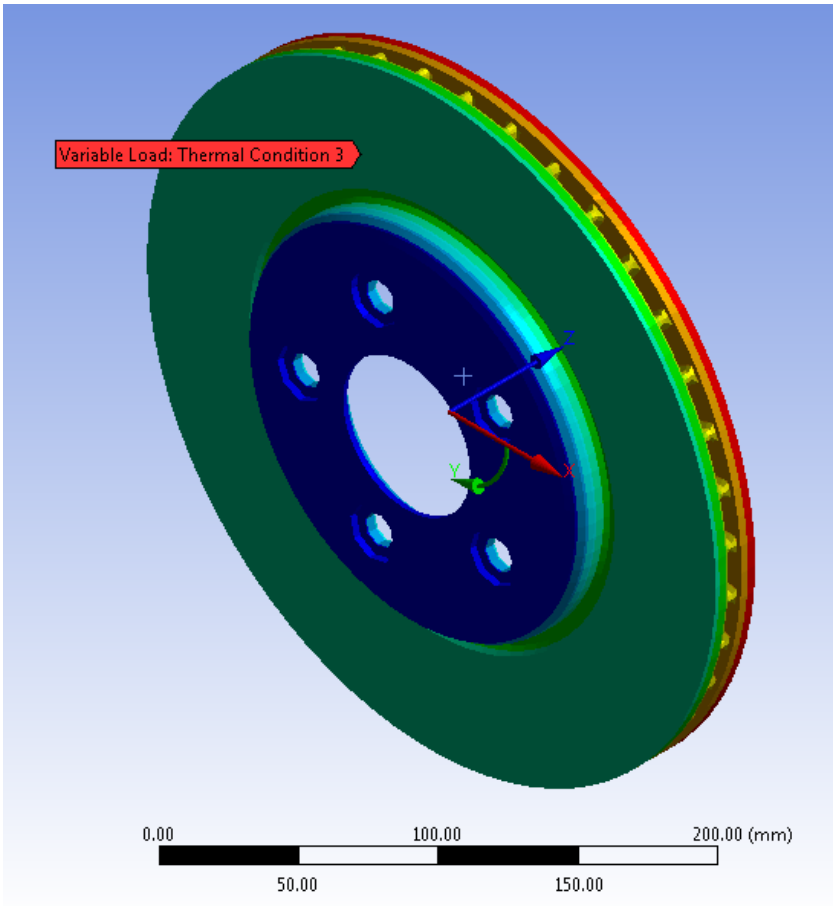

Figure 5-4: Linear temperature profile distribution in axial (thickness) direction.

CHAPTER SIX: COUPLING OF VIBRATION AND THERMAL BUCKLING ANALYSIS

6.1 Coupling overview and effect of vibration on thermal buckling

The coupling analysis of vibration and thermal buckling is a significant study to be conducted as there are various mechanical operations that can affect the critical buckling temperature of a brake disc, either increasing or decreasing the critical buckling temperature. As stated in an earlier chapter, vibration in a brake can occur during the rotation of the wheel, and at given speeds, the frequency of the vibration varies; at lower speeds, the frequency is higher compared to higher speeds. The coupling of vibration and thermal buckling occurs during braking. If there is vibration present during the rotation of the brake rotor, and the brakes are applied, the contact between the brake pads and rotor will be different from the case if there was no vibration present during the rotation of the rotor. It is known that heat generated during a sliding process depends on the coefficient of friction, sliding speed, applied force or pressure normal to surface and contact area between both surfaces.

For simplicity, in the previous chapter, the temperature distribution used was a generic assumption of linear profile. Also, for the sake of this thesis, it is assumed the sliding speed i.e., rotational speed of the brake rotor, coefficient of friction and brake force applied remain constant during the braking process with and without the presence

of vibration. Therefore, the only variable that changes in both scenarios (with or without vibration) is the contact area between the brake rotor and the pads. Figure 6-1 shows an image of a run-out error; that is when the brake disc is pulling out of alignment. In a situation where run-out error occurs, the heat generated is different and in turn the temperature profile in the brake rotor changes. In the previous chapter, the situation studied assumed no run-out error and simplified temperature profiles. This chapter studies the coupling between vibration and thermal buckling.

The coupling consists of three consecutive steps. The first step is obtaining the deformed result from the vibration simulation performed in ANSYS. This is achieved by exporting the deformation result in a text file. The text file consists of the node number, node xyz location in mm and the total deformation in mm. The second step is importing the text file in MATLAB and calculates for temperature using Equation 11. Plot temperature vs. location and using MATLAB curve fitting tool found in the apps menu, find a profile that best fits the plot and it automatically generates an equation. The third step is obtaining the equation from step 2 and apply a thermal load described by the function in the buckling analysis conducted in ANSYS.

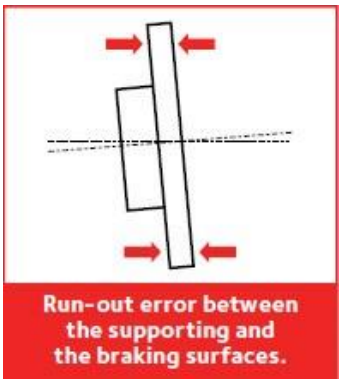

Figure 6-1: Run-out error [6]

Equation 10 shows the relationship of a simplified analysis between deformation and temperature change. Deformation is directly proportional to temperature change, where k is a constant. During braking, the temperature in the brake rotor can reach up to 800°C, and deformation can be very small, hence the multiplication of a constant with the deformation to increase the value of the change in temperature to match the high temperatures. To keep a constant maximum temperature with that used in the uncoupled thermal buckling analysis, the chosen constant for k, is determined by the maximum deflection from the vibration simulation. Therefore, the value k varies in such a way that the maximum temperature is 250°C. The maximum temperature used is a calculated average temperature obtained from Belhocine Ali, and Mostefa Bouchetara's [44] finding of temperatures through a disc thickness of three types of cast irons. To maintain the units for Equation 11, the value of k is multiplied by 1°C and divided by 1mm. Table 6-1 shows the value for k, based on the maximum directional deflection obtained from the mode 1 deformation in mm for each study conducted with the various rotational velocities. The direction of the applied thermal load is guided by the directional

deformation. Therefore, using the data obtained from the radial deformation to create a data set, creating a plot and finding the best fit for the plot and obtaining an equation; the equation used for the thermal load will be applied in the radial direction. Likewise, a temperature distribution in the axial direction is from data collected from the axial deformation. Figure 6-2 shows a plot of temperature vs. radial location with temperature calculated using the radial deformation data and Figure 6-3 shows a plot of temperature vs. axial location. Both plots follow the same profile as the deformation plot due to the relation stated in Equation 10 and the temperature is calculated using Equation 11. The maximum temperatures calculated using Equation 11 for the plot constructed in Figure 6-2 and Figure 6-3 are 250°C and the minimum calculated temperatures are -205.4543°C and -205.3615°C respectively.

$$\Delta T \propto k^{*}\Delta U \tag{10}$$

$$T = (k * U) + 22 \tag{11}$$

Table 6-1: Values of k based on the maximum radial deflection for each rotational velocity

Rotational Velocity [rad/s]	Maximum Radial Deflection [mm]	Value of k
14	5.6860	40.0985
32	5.2648	43.3065
43	5.1686	44.1125

Table 6-2: Values of k based on the maximum axial deflection for each rotational velocity

Rotational Velocity [rad/s]	Maximum Axial Deflection [mm]	Value of k
14	21.9790	10.3735
32	20.3530	11.2023
43	19.9820	11.4103

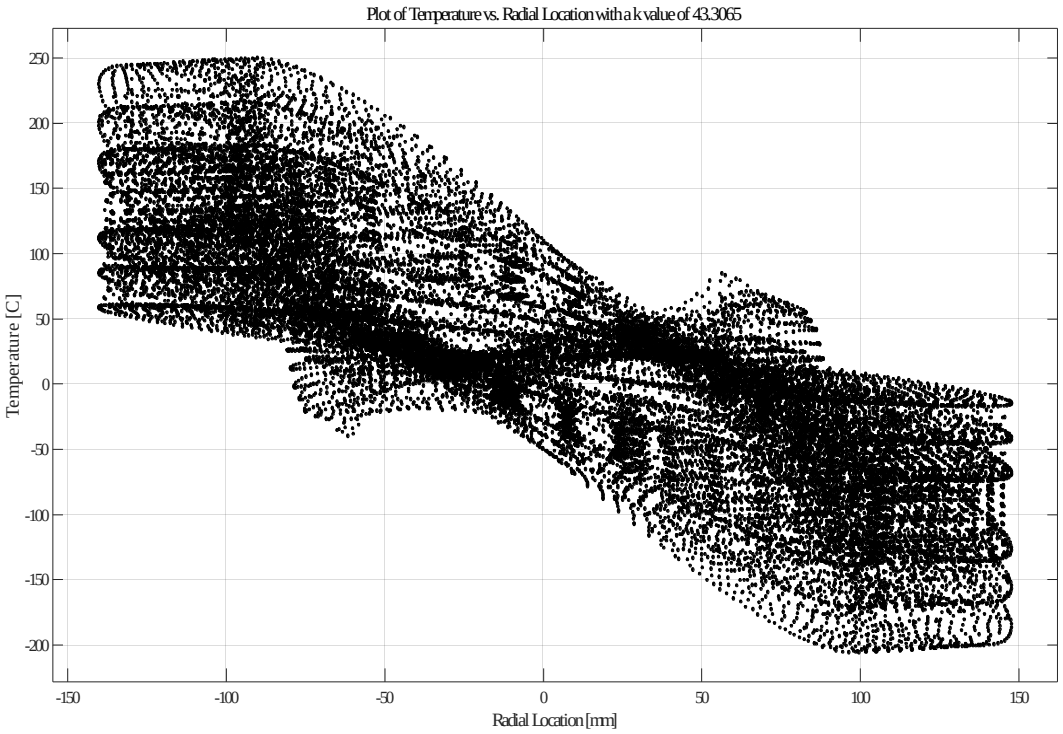

Figure 6-2: Plot of Temperature vs. Radial Location with a k value of 43.3065

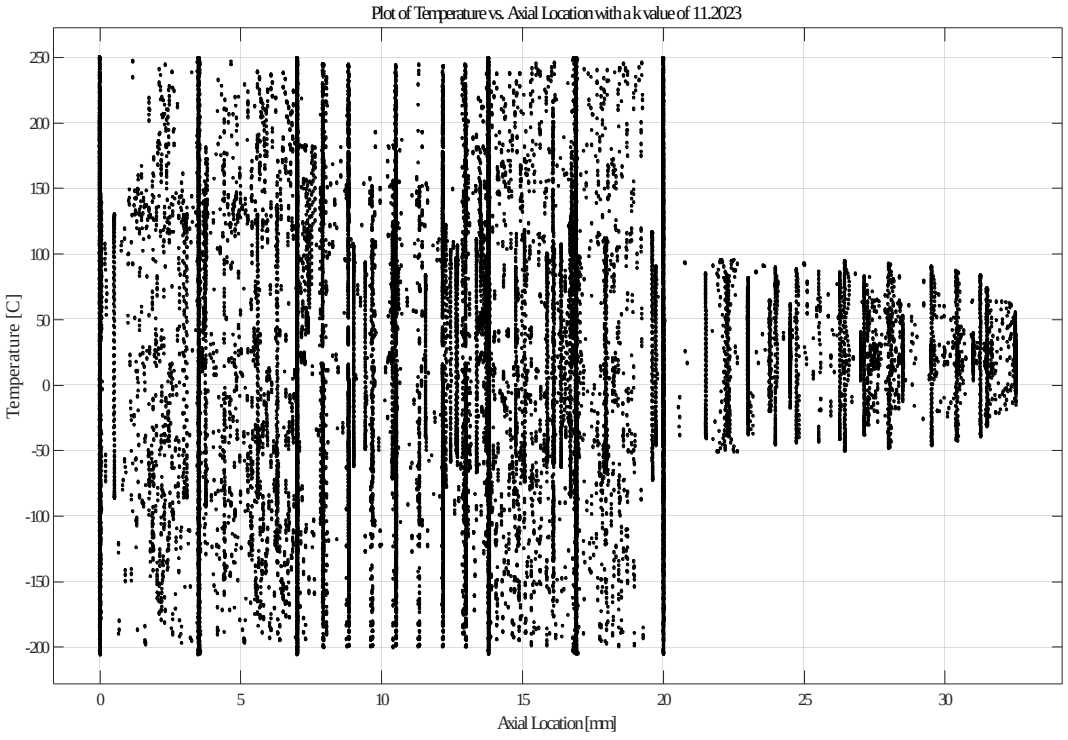

Figure 6-3: Plot of Temperature vs. Axial Location with a k value of 11.2023

Using MATLAB curve fitting tool, the best fit found for Figure 6-2 is a third degree polynomial equation and for Figure 6-3 a table was generated from MATLAB containing the temperatures and axial locations. Equation 12 shows the format of the equation of the best fit for Figures 6-2. The coefficients p1, p2, p3, and p4 were calculated and generated by MATLAB.

$$p1x^3 + p2x^2 + p3x + p4 \qquad (12)$$

The critical buckling temperature was calculated as the product of the load multiplier and the highest nodal temperature. Figure 6-4 shows the mode 1 total deformation in mm of the buckling analysis with a temperature profile governed by Equation 12 in the radial

direction with a maximum deflection of 1.04mm and Figure 6-4 is similar to that obtained for the mode 1 total deformation for a temperature profile governed by Equation 13 in the axial direction and the same maximum deflection of 1.04mm. The potato chip and coning modes were observed in modes 7 and 8 respectively for both temperature profiles in the radial and axial direction. The color scheme denotes the minimum and maximum deflection, blue being the minimum deflection and red being the maximum deflection. Table 6-3 shows the critical buckling temperature with the corresponding rotational velocities and a temperature profile governed by Equation 12 and distributed in the radial direction. Table 6-4 shows the critical buckling temperature with the rotational velocities and a temperature profile governed by Equation 13 distributed in the axial direction.

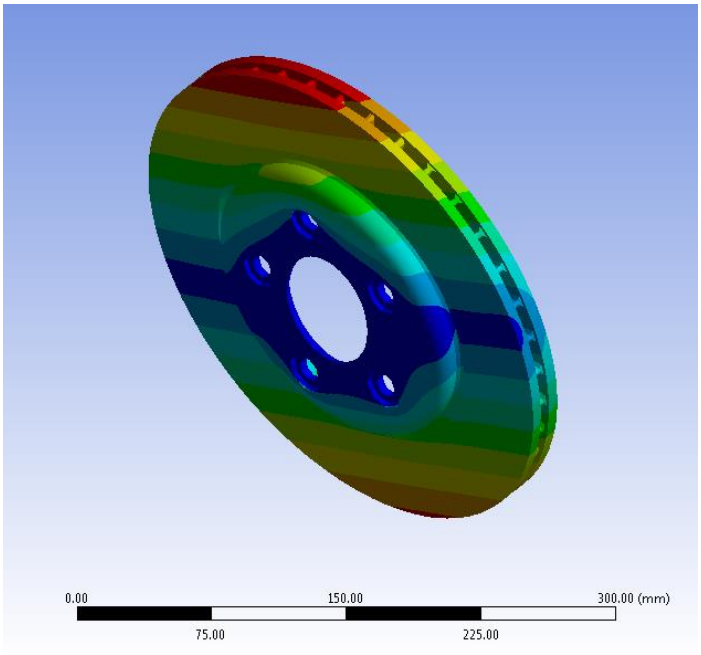

Figure 6-4: Mode 1 total deformation in mm of the coupled buckling analysis, with a temperature profile in the radial direction.

Table 6-3: Critical buckling temperature corresponding to the vibration observed at the various rotational velocities with applied thermal load in the radial direction.

Rotational Velocity [rad/s]	Maximum Deflection [mm]	Frequency [Hz]	Load Multiplier	Critical Buckling Temperature [°C]
14	5.6860	773.31	82.573	1.4238×10^4
32	5.2648	770.78	82.584	1.4240×10^4
43	5.1686	769.21	486.21	1.4241×10^4

Table 6-4: Critical buckling loads corresponding to the vibration observed at the various rotational velocities with applied thermal load in the axial direction.

Rotational Velocity [rad/s]	Maximum Deflection [mm]	Frequency [Hz]	Load Multiplier	Critical Buckling Temperature [°C]
14	21.9790	773.31	537.72	3.8005×10^4
32	20.3530	770.78	537.73	3.4784×10^4
43	19.9820	769.21	537.73	3.4769×10^4

6.2 Effect of critical thermal buckling temperature on vibration

In a coupling situation, the phenomenon coupled is suspected to influence each other. In this coupling of vibration and thermal buckling study, it is prudent to study the effect of vibration on thermal buckling, and how it affects the critical thermal buckling temperature, as well as the effect of thermal buckling on vibration, how the thermal buckling temperature affects the frequency of vibration and displacement. Figure 6-5 shows the vibration mode 1 total deformation in mm with a temperature profile in the radial direction and a critical buckling temperature of 1.4238×10^4 ºC. Table 6.5 shows the rotational velocity, frequency and maximum deflection correlated to the critical thermal buckling temperature. The maximum deflections shown in Table 6-5 are the deformations

obtained from the vibration simulation to verify if the critical buckling temperature does affect the frequency of vibration and the deformation during vibration.

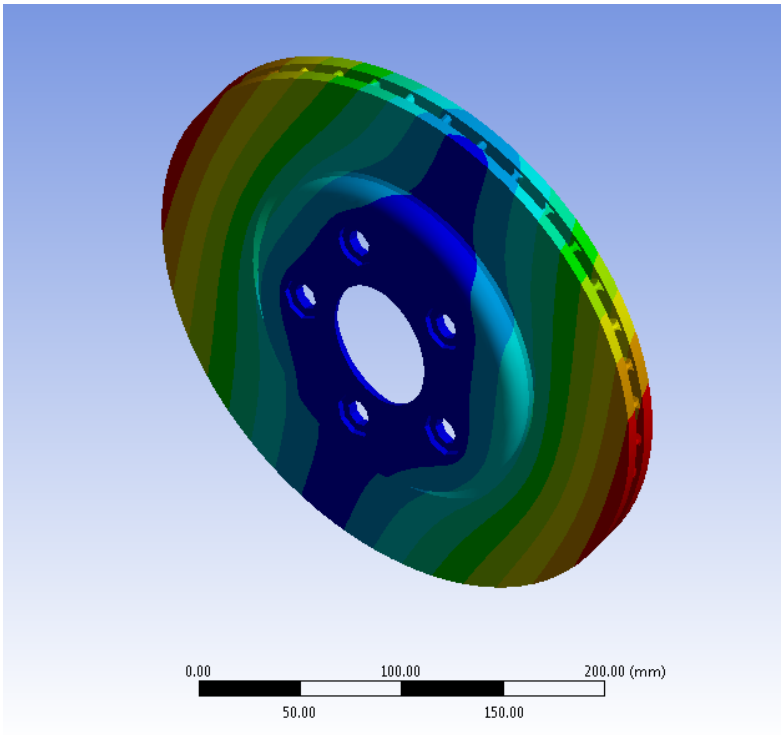

Figure 6-5: Total Deformation in mm of vibration mode 1 with critical buckling temperature of 1.4240×10^4 ºC and rotational vibration of 32rad/s

Table 6-5: Frequency and maximum deflection of vibration study with applied critical thermal buckling temperature.

Critical Buckling Temperature [°C]	Rotational Velocity [rad/s]	Frequency [Hz]	Maximum Total Deflection [mm]	Maximum Radial Deflection [mm]	Maximum axial Deflection [mm]
1.4238×10^4	14	773.31	22.6690	5.6860	21.9790
	32	770.78	20.9920	5.2648	20.3530
	43	769.21	20.6100	5.1686	19.9820
3.4784×10^4	14	773.31	22.6690	5.6860	21.9790
	32	770.78	20.9920	5.2648	20.3530
	43	769.21	20.6100	5.1686	19.9820

As seen in Figure 6-5 and Table 6-5, it can be noted that thermal buckling temperature has no effect on vibration. The frequency and maximum deflection remain the same as the results from the previous vibration analysis chapter. Therefore, with or without an applied temperature field, and with various applied temperature field, it shows in Table 6-5 that the frequency and maximum total and individual directional deflection are unaffected.

CHAPTER SEVEN: CONCLUSION AND FUTURE WORK

The critical buckling temperatures obtained from the coupling analysis are as high as the uncoupled buckling temperature. The critical buckling temperature in the coupling analysis is seen with a minimum value of 1.4238×10^4 °C with a temperature profile in the radial direction and 14 rad/s rotational velocity. This high value signifies that buckling is unlikely to occur, because the critical buckling temperature is higher than the melting point of gray cast iron. Also, it is concluded that buckling is unlikely to occur with the given conditions studied in Chapter 5 the uncoupled thermal buckling analysis, because, the critical buckling temperatures of 1.1607×10^4 °C, 1.5465×10^4 °C and 1.7098×10^4 °C are higher than the melting point of gray cast iron. Therefore, vibration during braking does not increase the chances of buckling in a brake disc with the chosen material, dimensions, and rotational velocity. It should be noted that the higher the temperature difference from the inner radius to the outer radius, the lower the buckling temperature. This only holds true with the chosen dimensions for the brake rotor in Table 3-1. As seen in the equations from Chapter 5, buckling is governed by a lot of variables such as material properties, geometric dimensions, and temperature changes. Changing these variables will show a noticeable change in the critical buckling temperature. This was proved in Tables 6-3 and 6-4, that changing the temperature profile, and also the thermal load direction does show a noticeable change in the critical buckling temperature. A more

realistic temperature profile for a thermal buckling analysis can be achieved with a transient dynamic analysis with all the brake components included in the analysis.

Axial run-out in a brake disc is a type of vibration induced phenomenon that was not studied in detail in the past. A coupling study with axial run-out should be studied more in the future, such as coupling between transient heat transfer and structural dynamics to better understand how this can affect the heat generation, heat dissipation, the wear rate of the brake pads and the structural integrity of the brake rotor.

Vibration in a brake disc can occur in a different number of ways such as low frequency vibration that occurs due to non-uniformity caused by “hot spots”. The localized hot and cold regions can be hypothesized that they cancel out each other and would not cause thermal buckling. However, in future research, a multistage coupling of thermoelastic instability, vibration, and thermal buckling should be analyzed to investigate the validity of this hypothesis in more depth.

REFERENCE

[1] Dimarogonas, A.d. “The Origins of Vibration Theory.” *Journal of Sound and Vibration*, vol. 140, no. 2, 1990, pp. 181–189., doi:10.1016/0022-460x(90)90523-3.

[2] Smith, George, "Newton's *Philosophiae Naturalis Principia Mathematica", The Stanford Encyclopedia of Philosophy* (Winter 2008 Edition), Edward N. Zalta (ed.), URL = <https://plato.stanford.edu/archives/win2008/entries/newton-principia/>.

[3] Newton, Isaac, *Philosophiae Naturalis Principia Mathematica* (“*Mathematical Principles of Natural Philosophy*”), London, 1687; Cambridge, 1713; London, 1726. (Pirated versions of the 1713 edition were also published in Amsterdam in 1714 and 1723.)

[4] Puhn, Fred. *Brake Handbook.* HP Books, 1985.

[5] Simulia, Inc. “ABAQUS/Explicit User’s Manual”. Version 6.13. Providence, RI, USA. (2017)

[6] “Basics of Vibration Analysis - Vibration Monitoring | Erbessd®.” *ERBESSD INSTRUMENTS*, 11 June 2019, www.erbessd-instruments.com/articles/vibration-analysis.

[7] Timošenko Stepan Prokof'evič, and James Monroe Gere. *Theory of Elastic Stability*. Dover Publ., 2009.

[8] Zhao, Jiaxin, et al. "Finite Element Analysis of Thermal Buckling in Automotive Clutch Plates." *Journal of Thermal Stresses*, vol. 39, no. 1, 2016, pp. 77–89., doi:10.1080/01495739.2015.1123590.

[9] Jones, Robert M. *Buckling of Bars, Plates, and Shells*. Bull Ridge Publ., 2006.

[10] Yi, Yun-Bo, et al. "Thermoelastic Instabilities in Automotive Disc Brakes — Finite Element Analysis and Experimental Verification." *Solid Mechanics and Its Applications Contact Mechanics*, 2002, pp. 187–202., doi:10.1007/978-94-017-1154-8_20.

[11] Kubota, Masahiro, et al. "A Study of the Mechanism Causing High-Speed Brake Judder." *SAE Technical Paper Series*, 1998, doi:10.4271/980594.

[12] "Brake Judder In Detail." *Replacement Car & Truck Brake Parts | Jurid Parts*, www.jurid.com/technical-support/light-vehicles/technical-tips/brake-judder.html.

[13] Ma, C. "Thermal buckling of automotive brake discs". Dissertation, University of Michigan.

[14] Maluf, Omar & Angeloni, Mauricio & Milan, M & Spinelli, Dirceu & Wladimir, Waldek & Filho, Bose. (2004). Development of materials for automotive disc brakes. Pesquisa Technol Minerva. 2.

[15] Bloch, Heinz P., and Fred K. Geitner. *Machinery Failure Analysis and Troubleshooting*. Butterworth-Heinemann, 2012.

[16] Boughner, Derek R., and Margot R. Roach. "Effect of Low Frequency Vibration on the Arterial Wall." *Circulation Research*, vol. 29, no. 2, 1971, pp. 136–144., doi:10.1161/01.res.29.2.136.

[17] Okamura, Toshikazu, and Hiroyuki Yumoto. "Fundamental Study on Thermal Behavior of Brake Discs." *SAE Technical Paper Series*, 2006, doi:10.4271/2006-01-3203.

[18] Tauchert, Theodore R. "Thermally Induced Flexure, Buckling, and Vibration of Plates." *Applied Mechanics Reviews*, vol. 44, no. 8, 1991, p. 347.

[19] Thornton, Earl A. "Thermal Buckling of Plates and Shells." *Applied Mechanics Reviews*, vol. 46, no. 10, 1993, p. 485.

[20] Daws, J. W., et al. "The Impact of Plus-Sized Wheel/Tire Fitment on Vehicle Stability4." *Tire Science and Technology*, vol. 35, no. 1, 2007, pp. 23–40., doi:10.2346/1.2698541.

[21] “Come to Us for Brake Service You Can Depend On.” *Integrity Auto Care*, 8 July 2019, stowintegrityauto.com/brake-service-can-depend/.

[22] Web Style Media, LLC. “Anatomy of Your Brakes: Car Care Articles.” *Sensible Driver*, sensibledriver.com/article/anatomy-of-your-brakes.

[23] Jin, T.l., et al. “A Study of the Thermal Buckling Behavior of a Circular Aluminum Plate Using the Digital Image Correlation Technique and Finite Element Analysis.” *Thin-Walled Structures*, vol. 77, 2014, pp. 187–197., doi:10.1016/j.tws.2013.10.012.

[24] Joubaneh, E Farzaneh, et al. “Thermal Buckling Analysis of Porous Circular Plate with Piezoelectric Sensor-Actuator Layers under Uniform Thermal Load.” *Journal of Sandwich Structures & Materials*, vol. 17, no. 1, 2014, pp. 3–25., doi:10.1177/1099636214554172.

[25] Ghiasian, S.e., et al. “Thermal Buckling of Shear Deformable Temperature Dependent Circular/Annular FGM Plates.” *International Journal of Mechanical Sciences*, vol. 81, 2014, pp. 137–148., doi:10.1016/j.ijmecsci.2014.02.007.

[26] Altuzarra, Oscar, et al. “Judder Vibration in Disc Brakes Excited by Thermoelastic Instability.” *Engineering Computations*, vol. 19, no. 4, 2002, pp. 411–430., doi:10.1108/02644400210430181.

[27] Ishihara, Noriyuki, et al. “Experimental Analysis of Low-Frequency Brake Squeal Noise.” *SAE Technical Paper Series,* 1996, doi:10.4271/962128.

[28] Kumemura, Yoichi, et al. “Analysis for Reducing Low Frequency Squeal of Disc Brake.” *SAE Technical Paper Series*, 2001, doi:10.4271/2001-01-3137.

[29] Nishiwaki, Masaaki, and Yukio Yamamoto. “A Study on Trigger of Small Friction Noise in Disc Brake Squeal.” *SAE Technical Paper Series*, 2018, doi:10.4271/2018-01-1872.

[30] Park, Jintack. “Design Optimization of the Disc Brake for Squeal Noise Reduction.” *SAE Technical Paper Series*, 2018, doi:10.4271/2018-01-1874.

[31] Bigoni, D., et al. “Effects of the Constraint's Curvature on Structural Instability: Tensile Buckling and Multiple Bifurcations.” *Proceedings of the Royal Society A: Mathematical, Physical and Engineering Sciences*, vol. 468, no. 2144, 2012, pp. 2191–2209., doi:10.1098/rspa.2011.0732.

[32] Ari-Gur, Judah, and Samuel R. Simonetta. “Dynamic Pulse Buckling of Rectangular Composite Plates.” *Composites Part B: Engineering*, vol. 28, no. 3, 1997, pp. 301–308., doi:10.1016/s1359-8368(96)00028-5.

[33] Zhao, Bo, et al. “The Effects of Thermo-Mechanical Load on the Vibrational Characteristics of Ultrasonic Vibration System.” *Ultrasonics*, vol. 98, 2019, pp. 7–14., doi:10.1016/j.ultras.2019.05.005.

[34] Stibich, Paul R., et al. “A Technique to Predict Thermal Buckling in Automotive Body Panels by Coupling Heat Transfer and Structural Analysis.” *SAE Technical Paper Series*, 2014, doi:10.4271/2014-01-0943.

[35] Pegg, N.g. “A Numerical Study of Dynamic Pulse Buckling of Ring-Stiffened Cylinders.” *Computers & Structures*, vol. 44, no. 6, 1992, pp. 1205–1214., doi:10.1016/0045-7949(92)90364-6.

[36] Hu, Shugen, and Yucheng Liu. “Disc Brake Vibration Model Based on Stribeck Effect and Its Characteristics under Different Braking Conditions.” *Mathematical Problems in Engineering*, vol. 2017, 2017, pp. 1–13., doi:10.1155/2017/6023809.

[37] Wellford, L.carter, and Ghassan M. Dib. “Finite Element Methods for Nonlinear Eigenvalue Problems and the Postbuckling Behavior of Elastic Plates.” *Computers & Structures*, vol. 6, no. 4-5, 1976, pp. 413–418., doi:10.1016/0045-7949(76)90020-1.

[38] Audebert, Nadine, et al. “Buckling Of Automatic Transmission Clutch Plates Due To Thermoelastic/Plastic Residual Stresses.” *Journal of Thermal Stresses*, vol. 21, no. 3, 1998, pp. 309–326., doi:10.1080/01495739808956149.

[39] Duan, C, and R Singh. “Analysis of the Vehicle Brake Judder Problem by Employing a Simplified Source—Path—Receiver Model.” *Proceedings of the*

Institution of Mechanical Engineers, Part D: Journal of Automobile Engineering, vol. 225, no. 2, 2011, pp. 141–149., doi:10.1177/09544070jauto1629.

[40] Jr, M. Triches, et al. "Reduction of Squeal Noise from Disc Brake Systems Using Constrained Layer Damping." *Journal of the Brazilian Society of Mechanical Sciences and Engineering*, vol. 26, no. 3, 2004, doi:10.1590/s1678-58782004000300011.

[41] Meyer, Ralf. "Brake Judder - Analysis of the Excitation and Transmission Mechanism within the Coupled System Brake, Chassis and Steering System." *SAE Technical Paper Series*, 2005, doi:10.4271/2005-01-3916.

[42] Hajnayeb, Ali, et al. "An Experimental and Theoretical Study on the Vehicle Brake Judder." *SAE Technical Paper Series*, 2012, doi:10.4271/2012-01-1820.

[43] Palmer, E, et al. "An Optimization Study of a Multiple-Row Pin-Vented Brake Disc to Promote Brake Cooling Using Computational Fluid Dynamics." *Proceedings of the Institution of Mechanical Engineers, Part D: Journal of Automobile Engineering*, vol. 223, no. 7, 2009, pp. 865–875., doi:10.1243/09544070jauto1053.

[44] Belhocine, Ali, and Mostefa Bouchetara. "Thermal Analysis of a Solid Brake Disc." *Applied Thermal Engineering*, vol. 32, 2012, pp. 59–67., doi:10.1016/j.applthermaleng.2011.08.029.